PROCEEDINGS, 51st Workshop on Geothermal Reservoir Engineering
Stanford University, Stanford, California, February 9-11, 2026
SGP-TR-230

The Transport of Heat in a Hydraulic Fracture Caused by a Variable Flowrate: A Reduced-Order Lauwerier/Gringarten Extended Model

Mauricio A. Rivas, Douglas Simpkins, Victoria McGuire and Lev Ring

515 West Greens Rd, Houston, Texas 77067

mauricio.rivas@sagegeosystems.com

Keywords: Geothermal systems, thermal transport, fully variable flowrate, Huff-n-Puff Operations, Lauwerier and Gringarten model, memory splitting, implicit upwind scheme

ABSTRACT

A reduced-order model for thermal transport through a single hydraulic fracture in hot dry rock is presented, allowing for fully variable flow rates, including flow reversals. This model extends the classical Lauwerier/Gringarten framework, which has served for decades as a reliable, conservative tool for estimating heat harvesting efficiency under the assumption of constant flow.

However, modern geothermal strategies – such as Huff-n-Puff methods, thermal storage or variable charging and discharging cycles designed to deliver flexible generation profiles for power-grid demand – require models that accommodate arbitrary, time-dependent flowrates and fracture apertures. The developed model simulates these complex operations by reducing the coupled heat-transport equations into a one-dimensional advection-memory equation. This approach enables the fast design and analysis of injection-backflow tests and evaluation of long-term thermal depletion without the computational burden of full-physics simulators. Crucially, the model accounts for time-dependent fracture apertures, enabling it to simulate the physical 'breathing' of fractures caused by pressure fluctuations during charging and discharging.

Finally, the applicability of the developed model is validated by first reproducing the test case presented in Juliusson and Horne (2012) and secondly by considering a test case that models Huff-n-Puff operations. The findings highlight that the reduced-order model is efficient, reliable and robust so that it may be used for stochastic or long-term simulations.

1. INTRODUCTION

Different methodologies have been developed for modeling the extraction of heat from fractured hot dry rock. These may include analytical models, reduced-order models, to full-physics simulators. For many years, the Lauwerier (1955) and Gringarten et al. (1975) framework have served as reliable, foundational tools to conservatively estimate heat harvesting efficiency in hot dry rock or Enhanced Geothermal Systems (EGS). These classic models, however, are fundamentally based on the assumption of constant flowrates where fluid circulates through the fracture system in a single flow direction.

Recent advancements in geothermal energy, such as those described in Rivas et al. (2024) or Ricks et al. (2022), have moved beyond steady-state circulation toward time-dependent flow rates. In some of these systems, charging and discharging cycles are performed by controlling the injection and production well flowrates and pressures to deliver flexible generation profiles in response to power-grid demands and time-shift energy at high round-trip efficiencies. In others that include Huff-n-Puff operations, fluid is injected into a fracture, allowed to heat up, and then produced back from the same injection point. Such methods require a new class of reduced-order models where the flowrate is an arbitrary function of time rather than a fixed value.

The necessity of these models is driven by the practical limitations of current software. Even today, advanced numerical simulation of highly coupled thermal, hydraulic, and mechanical (THM) problems, for instance in Rivas et al. (2025), is extremely time and resource demanding. These challenges are particularly acute when reservoir performance – specifically thermal depletion – must be evaluated over many years or decades. Full-physics solvers, while accurate, are often not feasible for millions of iterations required in stochastic simulations (such as Monte-Carlo) used to explore parameter sensitivity or estimate heat transport variables.

Various authors have attempted to extend the Lauwerier/Gringarten model to bridge this gap. For instance, Kocabas and Horne (1987), Kocabas (2012) and Juliusson and Horne (2012) analyzed single step-changes in flowrate, either for switching circulation rates or moving from injection to production. However, these solutions were still restricted to step-function type flow and typically utilized double Laplace transforms that require complex numerical inversion in real space.

This paper introduces a reduced-order model that allows for a fully variable flowrate and time-dependent aperture. We demonstrate that a convolution approach, where a memory kernel captures rock heat diffusion, can transform the extended Lauwerier/Gringarten equations into a one-dimensional advection-memory equation. To ensure numerical efficiency without the need for Laplace inversion, we present an implicit upwind scheme based on memory-splitting. This method divides history into *recent* and *older* memory, using history compression for the latter to enable the fast, conservative, and robust long-term simulations required for modern, grid-responsive geothermal systems. Validation of the memory-splitting implicit numerical method is done by reproducing the test case of Juliusson and Horne (2012) with a single step-change in injection flowrate when operating a single-fracture geothermal system and using COMSOL

Multiphysics as the full-physics simulator. A second test case is considered to emulate Huff-n-Puff operations of the single-fracture geothermal system. To show robustness of the memory Lauwerier/Gringarten model, the first test case is in the time scale of decades with a step-change type flow schedule, and the second test case is in the time scale of days with a hypothetical smooth sinusoidal flow schedule. Lastly, a Huff-n-Puff simulation similar to one in Rivas et al. (2025) is done in order to compare qualitatively with the solver in this previous work.

2. THE THERMAL TRANSPORT MODELS AND NUMERICAL METHODS

We consider heat transport in a single hydraulic fracture embedded in a hot, impermeable rock matrix. The fracture is long compared to its width w and height H, allowing a reduction to a one-dimensional model of fluid flow along the fracture length (the x axis shown in Figure 1).

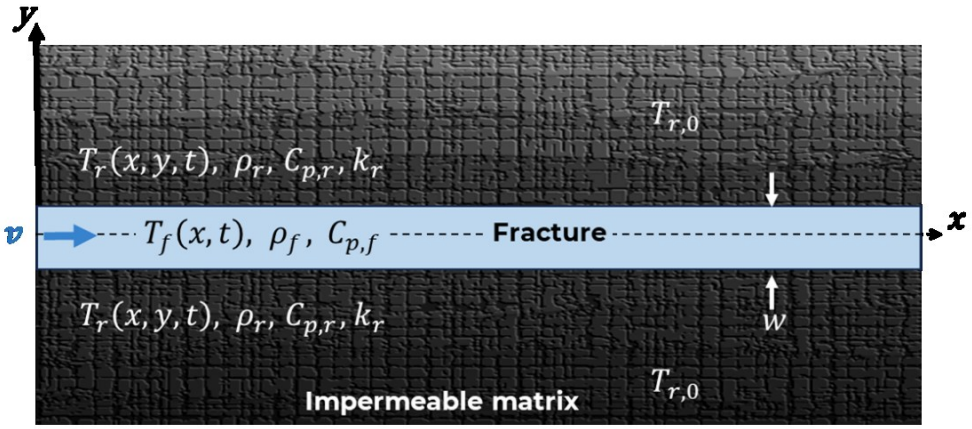

Figure 1: Schematic diagram of a single-fracture conceptual model.

The following assumptions are adopted:

(1) Single-phase slightly compressible liquid flow with constant density ρ_f and specific heat $C_{p,f}$.
(2) Uniform temperature across the fracture cross-section, so that the fluid temperature T_f varies only along the fracture length.
(3) Convection-dominated axial thermal transport in the fluid; axial thermal conduction in the fluid is neglected.
(4) Aperture can include spatial and temporal variations so that $w = w(x,t)$.
(5) Laminar flow with prescribed fracture volumetric flowrate $Q(x,t)$ that leads to the fluid velocity $v = Q/wH$.
(6) Semi-infinite rock on both sides of the fracture initially at uniform temperature $T_{r,0}$.
(7) Constant density ρ_r, specific heat $C_{p,r}$, and thermal conductivity k_r of the rock.
(8) Heat conduction in the x direction in the rock is neglected, so that the rock temperature T_r is one-dimensional at each x.
(9) Perfect thermal contact between the fluid and the fracture walls.
(10) No internal heat sources within the fluid.

2.1 The Memory Lauwerier/Gringarten Model that Includes a Variable Flowrate

Using Figure 1 to state the model, let x denote the fracture length coordinate and y the coordinate normal to the fracture wall. Heat conduction in the rock is governed by the one-dimensional diffusion equation at each x, while heat convection in the fluid is governed by advection with fluid velocity $v = v(x,t)$ that is allowed to be fully variable in both space and time which includes reversal of flow (i.e. flowback). The system of equations is:

$$\begin{cases} \dfrac{\partial T_r}{\partial t} = \alpha_r \dfrac{\partial^2 T_r}{\partial y^2} & \text{with} \quad y > 0 \\ \dfrac{\partial T_f}{\partial t} + v_{\text{eff}} \dfrac{\partial T_f}{\partial x} = \dfrac{k_r}{(\rho C_p)_{\text{eff}} w} \dfrac{\partial T_r}{\partial y}\Big|_{y=0} & \text{with} \quad x > 0 \end{cases} \tag{1}$$

where $\alpha_r := \dfrac{k_r}{\rho_r C_{p,r}}$ is the rock thermal diffusivity, $v_{\text{eff}} := \dfrac{\rho_f C_{p,f}}{(\rho C_p)_{\text{eff}}} v$ is the effective wave speed, and $(\rho C_p)_{\text{eff}} := \phi \rho_f C_{p,f} + (1-\phi)\rho_2 C_{p,2}$ the effective specific heat of the fracture with $\rho_2 C_{p,2}$ denoting either the volumetric specific heat of the proppant or of the rock and ϕ the porosity. The initial, interfacial, boundary and far-field conditions are:

$$\begin{cases} T_r(y,t=0) = T_f(x,t=0) = T_{r,0} \\ T_r(y=0,t) = T_f(x,t) \\ \begin{cases} T_f(x=0,t) = T_{inj} & \text{when } v > 0 \\ T_f(x=L,t) = T_{r,0} & \text{when } v < 0 \end{cases} \\ \lim_{y\to\infty} T_r(y,t) = T_{r,0} \end{cases} \tag{2}$$

where the constant $T_{r,0}$ is the initial temperature of the rock, T_{inj} is the constant temperature of the fluid being injected into the fracture at $x = 0, y = 0$ when the fluid velocity v is positive, and L is a length far away that the fluid does not reach; here, the dependence of T_r on the position x is suppressed.

Now, the flux at the fracture wall can be written exactly as a (memory operator) convolution using Green's function as:

$$q_{\text{wall}}(x,t) \coloneqq -k_r \left.\frac{\partial T_r}{\partial y}\right|_{y=0} = \frac{k_r}{\sqrt{\pi\alpha_r}} \int_0^t \frac{\partial T_f(x,t')}{\partial t'} \frac{dt'}{\sqrt{t-t'}} \tag{3}$$

where this expression captures the diffusive thermal penetration into the rock and introduces a non-local dependence on the temperature history; the derivation of this memory operator form of the flux is given in Appendix A. With this form of the flux, the system (1) reduces to the main equation:

$$\frac{\partial T_f}{\partial t} + v_{\text{eff}} \frac{\partial T_f}{\partial x} = -\frac{2k_r}{(\rho C_p)_{\text{eff}} w \sqrt{\pi\alpha_r}} \int_0^t \frac{\partial T_f(x,t')}{\partial t'} \frac{dt'}{\sqrt{t-t'}} \tag{4}$$

a one-dimensional advection-memory equation.

2.2 Analytical solution for constant velocity in Lauwerier/Gringarten model

To verify the numerical formulation, the special case originally analyzed by Lauwerier (1955) and Gringarten et al. (1975) for which a closed-form analytical solution exists is considered in this subsection. The assumptions there are that the velocity v is constant and so is the aperture w, as well as the physical properties $\rho_f, \rho_r, C_{p,f}, C_{p,r}, k_r$, and α_r. Moreover, it was assumed that the inlet temperature T_f is equal to the rock temperature $T_{r,0}$ at the initial time $t = 0$ and switches to a constant T_{inj} for $t > 0$. Under these assumptions, the original Lauwerier/Gringarten model can be rewritten as in equation (4), but with v_{eff} and w constant.

Introducing the retarded time coordinate and the temperature departure

$$\tau \coloneqq t - \frac{x}{v_{\text{eff}}} \quad \text{and} \quad \theta(\tau) \coloneqq T(\tau) - T_r \tag{5}$$

with the temperature remaining equal to the initial rock temperature $T_{r,0}$ for $\tau < 0$, the governing equation, for $\tau > 0$, reduces to an ordinary integro-differential equation in τ:

$$\frac{d\theta}{d\tau} = \frac{2k_r}{(\rho C_p)_c w \sqrt{\pi\alpha_r}} \int_0^\tau \frac{d\theta(\xi)}{d\xi} \frac{d\xi}{\sqrt{\tau-\xi}} \tag{6}$$

Lauwerier (1955) and Gringarten et al. (1975) showed, using double Laplace transforms, that the solution for the constant fluid velocity model is given by:

$$T(x,t) = T_{r,0} - \left(T_{r,0} - T_{inj}\right) \operatorname{erfc}\left(\frac{\sqrt{k_r \rho_r C_{p,r}}\, x/v_{\text{eff}}}{w \cdot (\rho C_p)_{\text{eff}} \cdot \sqrt{t - x/v_{\text{eff}}}}\right) \mathcal{H}(t - x/v_{\text{eff}}) \tag{7}$$

where $\operatorname{erfc}(\cdot)$ is the complementary error function and $\mathcal{H}(\cdot)$ is the Heaviside step function. An extended derivation of this analytical solution is presented in Juliusson and Horne (2012). This solution describes a thermally retarded advective front where heat exchange with the surrounding rock slows the propagation of the injected temperature signal relative to pure advection.

The Lauwerier-Gringarten solution provides an exact benchmark for validating numerical implementations of the advection-memory equation. In the present work, numerical results obtained using the implicit upwind finite-volume scheme with a split memory operator show excellent agreement with the analytical solution for both spatial temperature profiles and outlet temperatures histories.

2.3 The General Form of the 1D Advection-Memory Equation

Equation (4) is obtained from a conservative energy balance in the fracture. For a fracture of height $H(x)$ and aperture $w(x)$ that may vary spatially, the cross-sectional area is $A(x) = H(x)w(x)$. Averaging the energy equation over the fracture cross-section gives the following conservative balance:

$$\frac{\partial}{\partial t}\left(\left(\rho C_p\right)_{\text{eff}} HwT\right) + \frac{\partial}{\partial x}\left(\rho_f C_{p,f} QT\right) = 2Hq_{wall}(x,t) \tag{8}$$

where the factor of 2 accounts for heat loss through both fracture walls. Substituting the memory operator form of the flux from equation (3) gives:

$$\frac{\partial}{\partial t}\left(\left(\rho C_p\right)_{\text{eff}} HwT\right) + \frac{\partial}{\partial x}\left(\rho_f C_{p,f} QT\right) = -\frac{2Hk_r}{\sqrt{\pi a_r}} \int_0^t \frac{\partial T}{\partial t'} \frac{dt'}{\sqrt{t-t'}}. \tag{9}$$

This is the general form of the extended Lauwerier-Gringarten model.

For constant height H and aperture w, define the average fluid velocity as:

$$v(x,t) = \frac{Q(x,t)}{Hw}. \tag{10}$$

Dividing the conservative equation by $\left(\rho C_p\right)_{\text{eff}} Hw$ and simplifying leads to equation (4), which is a rewritten version of the classical Lauwerier-Gringarten 1D fracture heat transport equation. A key result is that the fracture height cancels identically, and heat loss depends only on the aperture w.

The model in (9) comprises an advective term and a non-local temporal memory operator representing rock heat conduction. The model is closed with initial condition

$$T(x,0) = T_{r,0} \tag{11}$$

and upwind boundary condition

$$\begin{cases} T(0,t) = T_{inj} & \text{if} \quad v(t) > 0 \\ T(L,t) = T_{r,0} & \text{if} \quad v(t) < 0 \end{cases} \tag{12}$$

where L is large enough that the fracture fluid front does not reach this length.

2.4 Numerical Discretization

The spatial domain is discretized using a finite-volume grid with cell centers x_i and walls $x_{i\pm1/2}$, whereas the advective flux is evaluated using a conservative upwind scheme based on the sign of the wall flowrate $Q_{i\pm1/2}$. This yields a tridiagonal linear system for the temperature at the new time step that can handle varying aperture, height, and flow magnitude and direction.

Since the convolution integral needs the whole history, it is split into recent and older time contributions. Over the most recent m time-steps, the integral is evaluated using exact quadrature weights:

$$\mathcal{I}_{\text{recent}} = \sum_{k=n-m}^{n} w_k (T^k - T^{k-1}) \quad \text{with} \quad w_k := \frac{2}{t^k - t^{k-1}} \left(\sqrt{t^n - t^{k-1}} - \sqrt{t^n - t^k}\right) \tag{13}$$

where $t^{k-1} < t^k < t^n$ follows a chosen time discretization. The last term $k = n$ depends on T^{n+1} and is treated implicitly, modifying the diagonal of the linear system and ensuring unconditional stability.

For times older than m time steps, the older history is compressed into a small number of decaying exponential *states* as in:

$$\frac{1}{\sqrt{t}} \approx \sum_{j=1}^{N_{\text{exp}}} a_j \, e^{-b_j t} \tag{14}$$

with each exponential arising from a state variable y_j satisfying the relation

$$\dot{y}_j = -b_j y_j + T'_{bdy} \tag{15}$$

The older time contribution to the convolution integral is

$$\mathcal{I}_{\text{older}} = \sum_{j=1}^{N_{\text{exp}}} a_j y_j \tag{16}$$

This compression allows to update the history with $O\left(N_{\text{exp}}\right)$ work instead of $O(N)$ where N is the number of time steps. The convolution integral is then the sum of these *recent* and *older* time contributions. This approach yields constant memory cost per cell while preserving long-time accuracy.

A classic problem in hydraulics in which there is a history integral (memory operator) at every time step was treated by Zielke (1968), and the solution of that hydraulic problem was improved by Trikha (1975) by using a short exponential series, and thus enabling recursive updates similar to the numerical discretization described above; see the work of Gao et al. (2022) on the sum-of-exponentials (SOE) algorithm for approximating kernels. Further details are provided in Appendix B below.

2.5 Fully Implicit Time Integration

Combining the spatial discretization with up-winding and the implicit part of the memory operator leads to a single tri-diagonal solve per time step that reads as:

$$\left(\frac{M_i}{\Delta t} + \text{Advection}_i - \frac{M_i}{\Delta t} c_i w_i\right) T_i^{n+1} = RHS \tag{17}$$

where RHS denotes the known right-hand side of the calculation and

$$c_i = -\frac{2k_r}{(\rho C_p)_{\text{eff}} w_i \sqrt{\pi \alpha_r}} \tag{18}$$

The advantages of this scheme are that it is conservative, unconditionally stable, efficient for long-time simulations and reproduces the classical analytical Lauwerier/Gringarten solution.

3. TEST CASES AND RESULTS OF THE MEMORY-SPLITTING NUMERICAL APPROACH

The memory-splitting implicit numerical method stated above for solving the 1D advection-memory equation (4) was implemented for three cases. These first and second cases were also solved using the finite element method (FEM), fully coupled, multi-physics simulator COMSOL to validate the memory-operator based approach and enable comparison with a full-physics numerical simulation. The third case was made to make a comparison with the simulator used in Rivas et al. (2025).

3.1 Single Step-Change in Injection Flowrate Test

For the first case, a test case given by Juliusson and Horne (2012) is reproduced here with parameter and operational values as in Table 1 for the physical model schematically given in Figure 1.

Table 1: Parameters for Case 1 simulations taken from Juliusson and Horne (2012).

Fracture Property	Unit	Value	Reservoir Property	Unit	Value
Aperture	mm	1	Matrix Porosity	$-$	0.001
Height	m	500	$T_{r,0}$	°C	150
Length	m	600	$(\rho C_p)_{rock}$	$\text{J/m}^3/°\text{C}$	2.5×10^6
Fracture Porosity	$-$	0.05	k_r	W/m/°C	3
Operational Parameter	**Unit**	**Value**	**Fluid Property**	**Unit**	**Value**
1st Flowrate before 3000 days	kg/s	28.9	T_{inj}	°C	50
2nd Flowrate after 3000 days	kg/s	17.4	k_f	W/m/°C	0.65
			$(\rho C_p)_f$	$\text{J/m}^3/°\text{C}$	4.2×10^6

As modeled in Juliusson and Horne (2012), this injection flowrate corresponds to $2{,}500\ m^3/\text{day}$ for the first 3,000 days and switches to $1{,}500\ m^3/\text{day}$ afterwards. A motivation for this case is the ability to assess the effects that a (single) change on injection flowrate has on the thermal recovery in a fractured geothermal system. Figure 2 shows the temperature coming out at the right-end of the fracture (in Figure 1) when the memory-splitting numerical approach and the COMSOL computations are implemented for this one step-change in flowrate test case.

These curves are comparable to the curves presented in Figure 3 of Juliusson and Horne (2012). Note that the time scale for this test case is in decades; for 8 years the geothermal operation injects at 28.9 kg/s into the fracture, and then the operation continues for another 19 years injecting at 17.4 kg/s. The simulations in Figure 2 show that this step-change in flowrate yields a rebound in production temperature and a smaller decay rate of the produced temperature for the subsequent 19 years.

It is seen from the numerical comparison in Figure 2 that the memory-splitting implicit numerical method accurately captures the fracture thermal transport before, during and after a sharp step-change of the injection flowrate. As was the case of the analytical model of Juliusson and Horne (2012), the memory-splitting model presented above can be used to optimize the injection schedule of the geothermal system of Figure 1 among the class of one-step-change schedules.

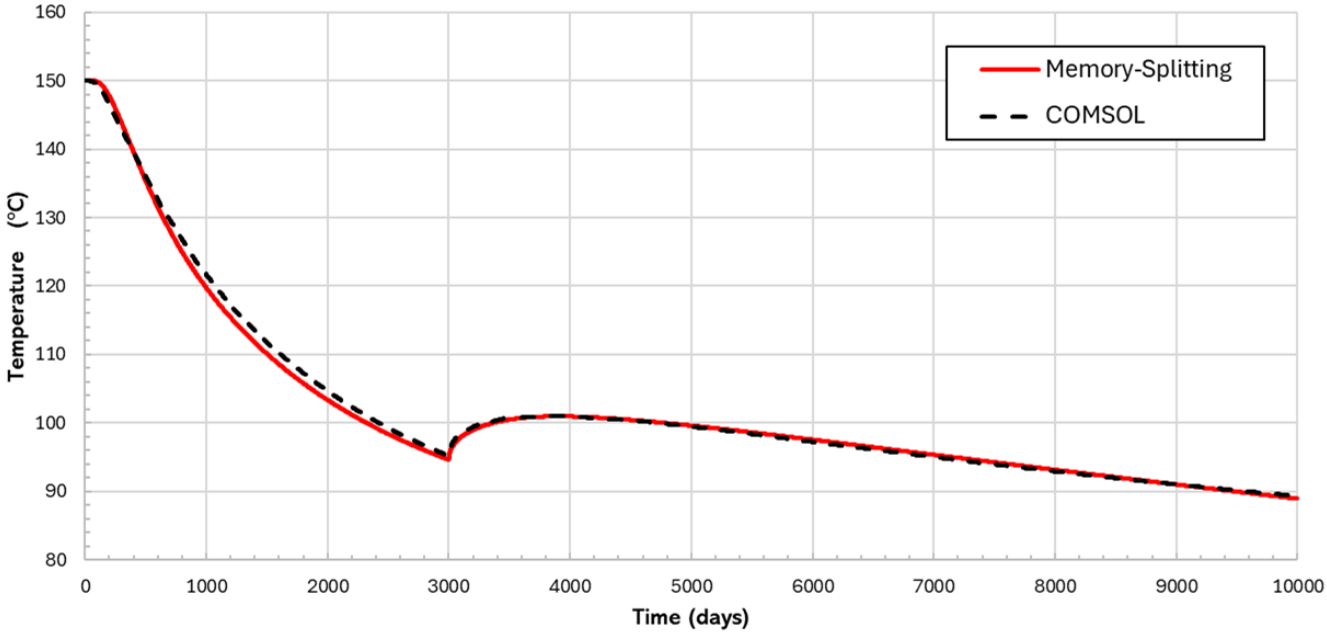

Figure 2: Comparing the memory-splitting numerical approach versus the COMSOL Multiphysics computation used for estimating fracture outlet temperature. The injection flowrate step-changes from 28.9 kg/s to 17.4 kg/s at day 3,000.

3.2 Fully Variable Injection Flowrate Test with Flowback

To exemplify the full capability of the memory-splitting approach, a fully variable injection flowrate schedule is used to assess the effect on the thermal recovery in a fractured geothermal system operated in a Huff-n-Puff manner. To do so, a hypothetical sinusoidal injection/production flowrate schedule at the fracture inlet, as given in Figure 3, is assumed for the geothermal system in Figure 1 where the point of injection and also production is the left endpoint of the fracture in Figure 1.

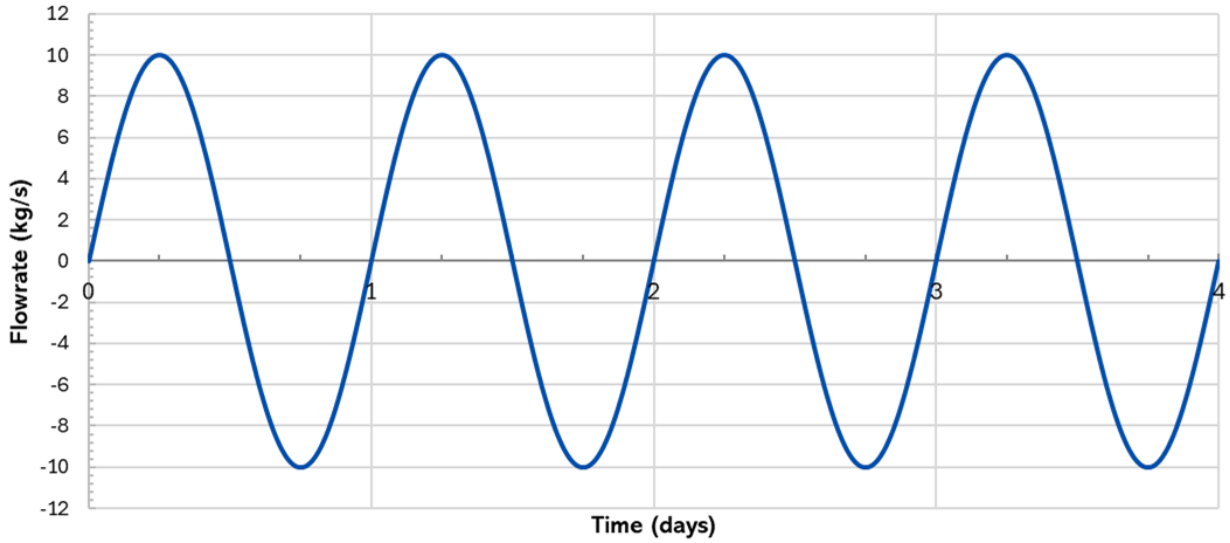

Figure 3: The fracture inlet flowrate schedule to emulate Huff-n-Puff operations on the geothermal system of Figure 1.

For this second test case, the time scale is chosen in days to further show the robustness of the memory-splitting methodology. During each of the four days, the injection flowrate increases from zero to 10 kg/s during the first 6 hours, and then decreases to zero by the 12th hour, always following the sinusoidal curve. After the 12th hour, the fracture is allowed to flow back through the same point of injection, with the flowback rate following exactly the negative part of the sinusoidal curve in Figure 3.

Figure 4 shows the temperature measured at the left endpoint of the fracture in Figure 1 when the memory-splitting numerical approach and the COMSOL computations are implemented for this Huff-n-Puff test case. The same thermophysical properties assumed for the first test case, recorded in Table 1, are assumed for this second test case.

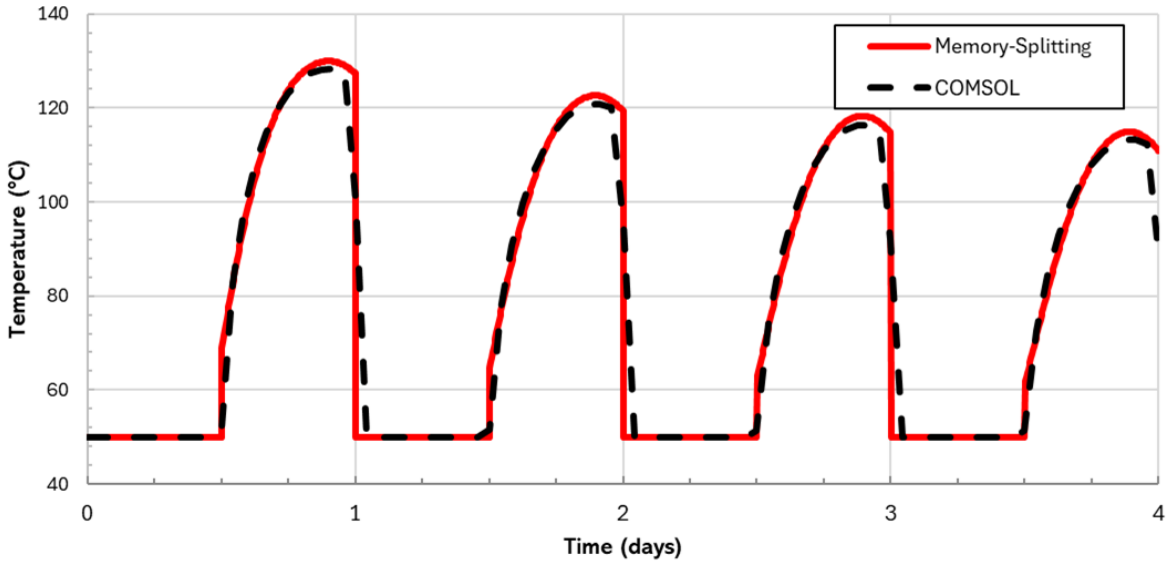

Figure 4: Comparing the memory-splitting numerical approach versus the COMSOL Multiphysics computation used for estimating fracture produced temperature when emulating Huff-n-Puff operations (following the schedule in Figure 3).

The results show that the temperature of the fluid injected at the left endpoint of the fracture is 50 °C during the first 12 hours of each day. When the fluid is produced from the fracture from the same fracture endpoint for the next 12 hours, the produced temperature increases until the flowrate reverses and fluid at 50 °C is injected back into the fracture for the following 12 hours. The maximum produced temperature is less for each consecutive cycle, but the decrease in max temperature is convex as similarly recorded in Rivas et al. (2025) using a different full-physics model with different parameters and cyclic flow schedule. The comparison with the COMSOL model in Figure 4 shows that also in the time scale of days, and with Huff-n-Puff (or fully variable flowrate with flowback) operations of the one-fracture geothermal system (in Figure 1), the memory-splitting implicit numerical method accurately captures the fracture thermal transport.

3.3 A Huff-n-Puff Test Similar to Previous Work

To compare the memory-splitting scheme with previous work, the reduced-order model parameters are updated with values that were used in Rivas et al. (2025), where the reservoir initially is at 200 °C. The pump schedule for each cycle is as follows: Inject fluid at 90 °C into the fracture for 10 hours; Produce the hot fluid for 10 hours. That is, the geothermal system is not shut-in, so it does not allow the cold fluid to *soak* with the hot fluid; this was the schedule for the simulation shown in Figure 5 of Rivas et al. (2025). Two cycles are simulated and the temperature at the fracture inlet/outlet is shown in Figure 5 below.

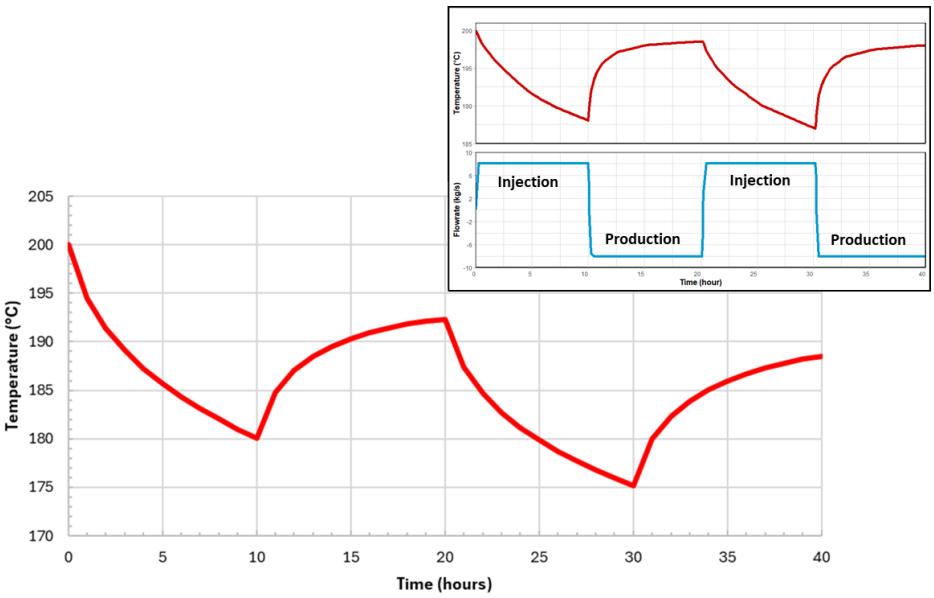

Figure 5: The memory-splitting model used for estimating produced fracture temperature from two Huff-n-Puff cycles. The inset plot shows the full-physics numerical result of a similar Huff-n-Puff operation from Figure 5 in Rivas et al. (2025).

The temperature profile generated by the reduced-order model follows the trend (red curve) seen in the full-physics model. Thus, additional processes would need to be incorporated into the reduced-order model to capture the proper physics

3.4 Discussion: Efficiency and Conservative Thermal Assessment

The comparative results between the memory-splitting reduced-order model and the COMSOL Multiphysics simulations confirm that this approach captures the critical thermal behavior of the system across vastly different time scales. While full-physics simulators account for complex thermo-hydro-mechanical (THM) couplings, this model provides a conservative estimation of heat harvesting efficiency by utilizing the established physics of the Lauwerier/Gringarten framework. Specifically, the accurate reproduction of the temperature *rebound* following flowrate changes in the case of subsection 3.1 and the cyclic decay in the case of subsection 3.2 illustrates that the memory-splitting method properly represents rock heat conduction without the computational overhead of solving high-dimensional coupled equations.

This efficiency is particularly vital when evaluating modern power-grid responsive operations, such as sinusoidal schedules used to emulate flexible generation profiles. Because the model accommodates time-dependent apertures $w = w(x, t)$, it is uniquely equipped to handle the physical *breathing* of fractures that occur during charging and discharging cycles. Ultimately, this reduced-order approach transforms the high-dimensional thermal transport problem into a manageable one-dimensional advection-memory equation. This transformation allows engineers to run the millions of iterations required for stochastic (or Monte-Carlo) simulations, ensuring that geothermal designs are both safe and highly optimized for modern power-grid flexibility demands.

4. CONCLUSION

This paper presents a robust reduced-order numerical model for thermal transport through a single hydraulic fracture that is specifically designed to meet the demands of modern geothermal operations. By extending the classical Lauwerier/Gringarten framework, the developed model transitions from steady-state assumptions to a dynamic system capable of handling fully variable injection and production flow rates.

Using a Laplace transform, the complex heat conduction process in the rock is converted into a convolution that transforms the system model into a one-dimensional advection-memory equation. This approach reduces the spatial dimension of the problem while accurately capturing diffusive thermal penetration. The numerical scheme avoids the computational bottleneck of Laplace inversion by splitting the temperature history into *recent* and *older* parts. The older memory is efficiently approximated via exponential modes, allowing for *aging* and *pushing* updates that significantly reduce computational costs. Unlike highly coupled thermal, hydraulic, and mechanical (THM) simulators, which are often too resource-intensive for long-term or stochastic assessments, this reduced-order model provides the speed necessary for evaluating thermal depletion over decades.

The model was validated against the benchmark case of Juliusson and Horne (2012) and full-physics COMSOL Multiphysics simulations. Results demonstrate that the method remains accurate across multiple time scales, from decades-long circulation to days-long sinusoidal Huff-n-Puff cycles. Ultimately, this model serves as a high-performance tool for designing geothermal systems that respond to fluctuating power-grid demands. By enabling the millions of iterations required for stochastic simulations, it provides a conservative and reliable pathway for optimizing heat extraction and ensuring the long-term sustainability of flexible geothermal generation.

REFERENCES

Gao, Z., Liang, J., and Xu, Z.: A Kernel-Independent Sum-of-Exponentials Method, J. Sci. Comput. **93**, 40 (2022).

Gringarten, A.C., Witherspoon, P.A. and Ohnishi, Y.: Theory of Heat Extraction from Fractured Hot Dry Rock, J. Geophys. Res., 80(8), 1120-1124 (1975).

Juliusson, E. and Horne, R.N.: Analytical Model for Thermal Response in a Fracture Due to a Change in Flow Rate, GRC *Transactions*, Vol. 36 (2012).

Kocabas, I.: Designing Thermal and Tracer Injection Backflow Tests, Proceedings World Geothermal Congress 2010, Bali, Indonesia, 25-29 April (2010).

Kocabas, I and Horne, R.N.: Analysis of Injection-Backflow Tracer Tests in Fractured Geothermal Reservoirs, Proceedings, 12th Workshop on Geothermal Reservoir Engineering, Stanford University, Stanford, CA (1987).

Lauwerier, H.A.: The Transport of Heat in an Oil Layer Caused by the Injection of Hot Fluid, Applied Scientific Research, 5(2) (1955).

Ricks, W., Norbeck, J. and Jenkins, J.: The Value of In-Reservoir Energy Storage for Flexible Dispatch of Geothermal Power, *Applied Energy*, vol. 313, no. C, Mar. (2022).

Rivas, M.A., McGuire, V., Simpkins, D. and Ring, L.: Geopressured Geothermal Systems: An Efficient and Sustainable Heat Extraction Method, *GRC Transactions*, Vol. 48 (2024).

Rivas, M.A., Simpkins, D., McGuire, V. and Ring, L.: Dynamics of Thermal Migration in Pressure-Propped Fractures During Huff-n-Puff Operations, Proceedings, 50th Workshop on Geothermal Reservoir Engineering, Stanford University, Stanford, CA (2025).

Trikha, A.K., An Efficient Method for Simulating Frequency-Dependent Friction in Transient Liquid Flow, ASME. J. Fluids Eng. 97(1): 97-105 (1975)

Zielke, W.: Frequency-Dependent Friction in Transient Pipe Flow, ASME. J. Basic Eng. 90(1): 109-115 (1968).

APPENDIX A: MEMORY OPERATOR THAT CAPTURES ROCK HEAT CONDUCTION

Here we derive the equivalent convolution representation of the heat flux through the fracture wall. By fixing the x coordinate and suppressing it in the following formulation, and letting y denote the coordinate perpendicular to the fracture face, i.e. into the rock as above, the corresponding semi-infinite domain heat equation is given by

$$\begin{cases} \frac{\partial T_r}{\partial t} = \alpha_r \frac{\partial^2 T_r}{\partial y^2} \\ T_r(y, t=0) = T_{r,0} \\ T_r(y=0, t) = T_{bdy}(t) \\ \lim_{y\to\infty} T_r(y,t) = T_{r,0} \end{cases} \tag{A1}$$

where $T_{bdy}(t)$ is a given temperature function at the boundary point $y = 0$. By taking Laplace transforms, the partial differential equation is transformed into the following ordinary differential equation

$$\alpha_r \frac{\partial^2 \hat{T}_r}{\partial y^2} - s\hat{T}_r = -T_{r,0} \tag{A2}$$

where $\hat{T}_r(y,s) = \mathcal{L}\{T_r(y,t)\}$ is the Laplace transform of T_r with respect to the time variable, and the initial condition is utilized. Imposing the boundary and far-field condition, this differential equation has the solution, in the Laplace space, given by

$$\hat{T}_r(y,s) = \frac{T_{r,0}}{s} + \left(\hat{T}_{bdy}(s) - \frac{T_{r,0}}{s}\right) e^{-y\sqrt{s/\alpha_r}} \tag{A3}$$

Now take the Laplace transform of the interface flux into the rock $q_{wall}(t) \coloneqq -k_r \frac{\partial T_r}{\partial y}\Big|_{y=0}$ and use (A3) to get

$$\hat{q}_{wall}(s) = -k_r \frac{\partial \hat{T}_r}{\partial y}\Big|_{y=0} = k_r \left(\hat{T}_{bdy}(s) - \frac{T_{r,0}}{s}\right)\sqrt{s/\alpha_r} \tag{A4}$$

Using the following basic results of Laplace transforms

$$\mathcal{L}\left\{\frac{1}{\sqrt{\pi t}}\right\} = \frac{1}{\sqrt{s}} \quad \text{and} \quad \mathcal{L}\left\{\int_0^t \frac{f'(t')}{\sqrt{\pi(t-t')}} dt'\right\} = \sqrt{s}\hat{f}(s) - \frac{f(0)}{\sqrt{s}} \tag{A5}$$

with $f(t) = T_{bdy}(t)$ in the second relation enables taking the inverse Laplace transform of (A4) to get

$$q_{wall}(t) = \frac{k_r}{\sqrt{\pi\alpha_r}} \int_0^t \frac{T'_{bdy}(t')}{\sqrt{t-t'}}\, dt' \tag{A6}$$

which is the desired reformulation for the wall heat flux (note that $T_{bdy}(t) \equiv T_f(x,t)$ in the general fracture heat transfer problem).

APPENDIX B: NUMERICAL APPROXIMATION OF THE MEMORY OPERATOR

To discretize the memory operator in (A6), let $0 = t^0 < t^1 < \cdots < t^{n-1} < t^n$ be a discrete set of times and define

$$\beta \coloneqq \frac{k_r}{\sqrt{\pi\alpha_r}}, \quad T^k_{bdy} \coloneqq T_{bdy}(t^k), \quad \Delta T^k_{bdy} \coloneqq T^k_{bdy} - T^{k-1}_{bdy}, \quad \Delta t^k \coloneqq t^k - t^{k-1}, \quad s_k \coloneqq \frac{\Delta T^k_{bdy}}{\Delta t^k}. \tag{B1}$$

Approximating by a piecewise-constant slope s_k on each interval $(t^{k-1}, t^k]$, the memory operator is estimated by

$$q^n_{wall} = \beta \sum_{k=0}^{n} s_k 2\left(\sqrt{t^n - t^{k-1}} - \sqrt{t^n - t^k}\right). \tag{B2}$$

For large times, this can become expensive to evaluate, but it is worth noting that terms near the current time have a stronger effect on the current time solution than terms further in the past. Therefore, the memory operator is split into a 'recent-part' and an 'older-part' where the history is split at a moving *cutoff time* t^c with $c < n$, as described next.

The Recent Part: This part integrates using the exact kernel over the interval $(t^c, t^n]$ to give

$$q^n_{\text{recent}} = \beta \sum_{k=c+1}^{n} s_k 2\left(\sqrt{t^n - t^{k-1}} - \sqrt{t^n - t^k}\right) \tag{B3}$$

so that this is a truncation of (B2).

The Older Part: This part represents the contribution from the past $[0, t^c]$ using states that are updated by 'pushing' one time-step's increment from the recent part into the older part at each time step.

First, fit for the kernel on the older time window $[0, t^c]$ to get

$$\frac{1}{\sqrt{t}} \approx \sum_{j=1}^{N} a_j e^{-b_j t} \quad \text{for } t \geq t_0 \tag{B4}$$

for some small positive value t_0, and define the *states* y^n_j at the n^{th} time step as

$$y^n_j \coloneqq \int_0^{t^c} T'_{bdy}(t') e^{-b_j(t^n - t')}\, dt' \tag{B5}$$

Then the older part is defined as

$$q^n_{\text{older}} \coloneqq \beta \sum_{j=1}^{N} a_j\, y^n_j \tag{B6}$$

To update the memory operator as time increases, the recent and older parts are updated as follows. Consider going from time t^n to time t^{n+1} so that the time step is Δt^{n+1}. First, update any states already in the older part by multiplying by the corresponding factor $e^{-b_j \Delta t^{n+1}}$:

$$y^{n+1}_j \quad \leftarrow \quad e^{-b_j \Delta t^{n+1}} y^n_j \tag{B7}$$

This is called *aging* of the existing older history. Next, the contribution from the recent part, at time t^n, to y^{n+1}_j is

$$\Delta y^{n+1}_{j,push} = \int_{t^c-1}^{t^c} s_c\, e^{-b_j(t^{n+1} - t')} dt' = s_c \cdot \frac{e^{-b_j(t^{n+1} - t^c)} - e^{-b_j(t^{n+1} - t^{c-1})}}{b_j}, \tag{B8}$$

and this gets *pushed* into the older part. The full update to the older part then reads as

$$y^{n+1}_j \quad = \quad e^{-b_j \Delta t^{n+1}} y^n_j + \chi_{c>0} \cdot s_c \cdot \frac{e^{-b_j(t^{n+1} - t^c)} - e^{-b_j(t^{n+1} - t^{c-1})}}{b_j}, \tag{B9}$$

where $\chi_{c>0}$ is a control equal to 0 or 1 that indicates to 'push' only when the recent time buffer is 'full'. The solution strategy for the memory operator is summarized in the following algorithm:

Inputs: c (recent time steps), arrays a_j, b_j, time grid t^k, temperatures T^k_{bdy}.

State y_j for $j = 1 \ldots N$, and a buffer storing the last c slopes s_k and their time indices.

For time step $n+1$:

1. Compute slope $s_{n+1} = \frac{T_{bdy}^{n+1} - T_{bdy}^{n}}{\Delta t^{n+1}}$ and push into buffer.
2. Evaluate the Recent Part: $q_{\text{recent}}^{n+1} = \beta \sum_{k=c+1}^{n+1} s_k \cdot 2\left(\sqrt{t^{n+1} - t^{k-1}} - \sqrt{t^{n+1} - t^{k}}\right)$.
3. Age the existing Older Part: for each mode j do: $y_j^{n+1} \leftarrow e^{-b_j \Delta t^{n+1}} y_j^n$.
4. Push the oldest step in the buffer into the Older Part (when $c > 0$): $y_j^{n+1} \leftarrow y_j^{n+1} + s_c \left(\frac{e^{-b_j (t^{n+1} - t^{c})} - e^{-b_j (t^{n+1} - t^{c-1})}}{b_j} \right)$.
5. Compute the Older Part: $q_{\text{older}}^{n+1} = \beta \sum_j a_j y_j^{n+1}$.
6. Compute the Total flux: $q_{wall}^{n+1} = q_{\text{recent}}^{n+1} + q_{\text{older}}^{n+1}$.

APPENDIX C: FITTING THE MEMORY KERNEL BY EXPONENTIALS

To see why fitting the memory kernel $K(t) \coloneqq 1/\sqrt{t}$ as given in (B4) is advantageous, substitute (B4) into the (memory operator) convolution integral to get

$$\int_0^t T'_{bdy}(t') K(t - t') dt' \approx \sum_{j=1}^{N} a_j \int_0^t T'_{bdy}(t') e^{-b_j (t - t')} dt' =: \sum_{j=1}^{N} a_j \, y_j \tag{C1}$$

Since differentiating the convolution y_j with respect to time gives the relation

$$\dot{y}_j = -b_j y_j + T'_{bdy}(t) \tag{C2}$$

it follows that y_j can be recursively updated at each time step so that there is no need for a full history storage.

The memory kernel approximation is summarized in the following algorithm where the notation $K(r) \coloneqq K(t - t')$ is used:

1. Choose the fitting window $[r_{\min}, r_{\max}]$ where:
   a. $r_{\min} > 0$ is how far back in time is considered to be no longer in the recent time.
   b. $r_{\max}$ is how far back in time is the corresponding history influential to the solution.
2. Choose log-spaced decay rates b_j to capture long times with $b_j \in \left[\frac{c_1}{r_{\max}}, \frac{c_2}{r_{\min}}\right]$ with c_1, c_2 in the order of 1 to 10.
   a. b_j on the smaller end leads to slowly decaying exponentials that capture longer histories.
   b. b_j on the higher end leads to fast decaying exponentials that capture shorter older behavior.
3. Build a sample grid in time by
   a. choosing log-spaced sample points $r_i \in [r_{\min}, r_{\max}]$ where $r_i \coloneqq r_{\min} \left(\frac{r_{\max}}{r_{\min}}\right)^{(i-1)/(M-1)}$ for $i = 1 \ldots M$;
   b. compute the target values $K_i = K(r_i) = \frac{1}{\sqrt{r_i}}$ for $i = 1 \ldots M$.
4. Solve for the coefficients a_j using least squares:
   a. Fix the decay rates b_j and set $K(r_i) \approx \sum_{j=1}^{N} a_j \, e^{-b_j r_i}$.
   b. This system is linear in a_j, so define the matrix $A_{ij} \coloneqq e^{-b_j r_i}$ and the vector $k_i = K(r_i)$.
   c. Solve the minimization problem: $\min_a \| W(Aa - k) \|_2$, where the weight W may be chosen to be
      i. a relative-error weighting as in $W_{ii} = \frac{1}{K(r_i)}$ to minimize relative error over long times
      ii. log-domain fitting with similar effects.

A constraint that may be imposed is for the a_j to be positive for all j as the kernel is positive and should be approximated by positive modes. This often improves stability and reduces cancellation errors in the tail.